

NO-A190 125

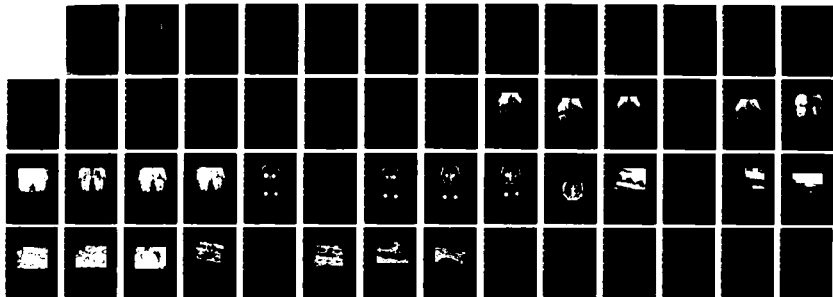
MANAGEMENT OF HARD TISSUE AVULSIVE WOUNDS AND
MANAGEMENT OF DROFACIAL FRACTURES(U) BATTELLE COLUMBUS
DIV OH C R HASSLER 16 OCT 87 DADA17-69-C-9118

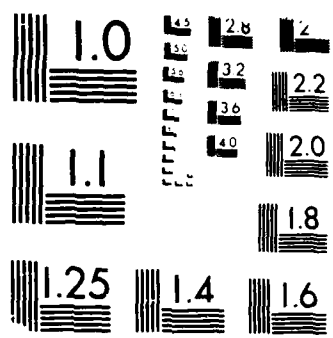
1/1

UNCLASSIFIED

F/G 6/5

ML





MICROCOPY RESOLUTION TEST CHART
NATIONAL BUREAU OF STANDARDS-1963-A

AD-A190 125

DTIC FILE COPY

2

AD _____

MANAGEMENT OF HARD TISSUE AVULSIVE WOUNDS
AND MANAGEMENT OF OROFACIAL FRACTURES

FINAL REPORT

Craig R. Hassler

October 16, 1987

DTIC
ELECTE
JAN 13 1988
S D

Supported by

U.S. ARMY MEDICAL RESEARCH AND DEVELOPMENT COMMAND
Fort Detrick, Frederick, Maryland 21701-5012

Contract Nos. DAMD17-82-C-2168
and DADA17-69-C-9118

BATTELLE
Columbus Division
505 King Avenue
Columbus, Ohio 43201-2693

DOD DISTRIBUTION STATEMENT

Approved for public release; distribution unlimited

The findings in this report are not to be construed
as an official Department of the Army position unless
so designated by other authorized documents.

019012

REPORT DOCUMENTATION PAGE				Form Approved OMB No 0704-0188 Exp Date Jun 30 1986	
1a REPORT SECURITY CLASSIFICATION Unlimited		1b RESTRICTIVE MARKINGS			
2a SECURITY CLASSIFICATION AUTHORITY		3 DISTRIBUTION / AVAILABILITY OF REPORT Approved for public release; distribution unlimited			
2b DECLASSIFICATION / DOWNGRADING SCHEDULE					
4 PERFORMING ORGANIZATION REPORT NUMBER(S)		5. MONITORING ORGANIZATION REPORT NUMBER(S)			
6a. NAME OF PERFORMING ORGANIZATION BATTELLE Columbus Laboratories		6b. OFFICE SYMBOL (if applicable)	7a. NAME OF MONITORING ORGANIZATION		
6c. ADDRESS (City, State, and ZIP Code) 505 King Avenue Columbus, Ohio 43201		7b. ADDRESS (City, State, and ZIP Code)			
8a. NAME OF FUNDING / SPONSORING ORGANIZATION U.S. Army Medical Research & Development Command		8b. OFFICE SYMBOL (if applicable)	9. PROCUREMENT INSTRUMENT IDENTIFICATION NUMBER DADA17-69-C-9118* DAMD17-82-C-2168		
8c. ADDRESS (City, State, and ZIP Code) Fort Detrick, Frederick, Maryland 21701-5012		10. SOURCE OF FUNDING NUMBERS			
		PROGRAM ELEMENT NO. 62775A	PROJECT NO 3S162, 775A825	TASK NO AA	WORK UNIT ACCESSION NO 044
11 TITLE (Include Security Classification) (U) Management of Hard Tissue Avulsive Wounds and Management of Orofacial Fractures					
12 PERSONAL AUTHOR(S) Craig R. Hassler, Ph.D.					
13a TYPE OF REPORT Final		13b TIME COVERED FROM 4/1/69 TO 4/30/85	14 DATE OF REPORT (Year, Month, Day) 1987 Oct 16		15 PAGE COUNT 53
16 SUPPLEMENTARY NOTATION *Includes Final for period of time April 1, 1969 - May 30, 1982 for Contract DADA17-69-C-9118.					
17 COSATI CODES			18 SUBJECT TERMS (Continue on reverse if necessary and identify by block number)		
FIELD	GROUP	SUB-GROUP	Bioceramics	Prosthetic Materials	Avulsive Wounds
06	03		Ceramic Implants	Implant Materials	Porous Ceramics
06	02		Biomaterials	Maxillofacial	Calcium Phosphates
19 ABSTRACT (Continue on reverse if necessary and identify by block number)					
<p>This final report outlines a study to investigate bioresorbable ceramics for the management of hard tissue avulsive wounds and orofacial fractures. The study spans a long time period, and consequently, includes several innovations and changes in project direction.</p> <p>The initiation portion of the study was the development and subsequent evaluation of numerous granular forms of ceramic materials that might potentially be biodegradable, osteophilic, and biocompatible. Numerous materials were prepared and implanted. The initial implant studies were performed at the U.S. Army Institutes of Dental Research. These initial studies indicated that tricalcium phosphate was a manufacturable and bioresorbable ceramic worthy of further development.</p>					
20 DISTRIBUTION / AVAILABILITY OF ABSTRACT <input type="checkbox"/> UNCLASSIFIED/UNLIMITED <input checked="" type="checkbox"/> SAME AS RPT <input type="checkbox"/> DTIC USERS			21 ABSTRACT SECURITY CLASSIFICATION		
22a NAME OF RESPONSIBLE INDIVIDUAL Mrs. Judy Pawlus		22b TELEPHONE (Include Area Code) 301-663-7325		22c OFFICE SYMBOL SGRD-RMI-S	

19. (Continued)

In addition to granular materials, calcium phosphates were developed in large segments. Materials ranging from fully dense to high-porosity materials were developed and evaluated in numerous animal models. Pore structure and chemical composition, as well as pore directionality, were extensively evaluated. Various manufacture methods were evaluated. The most reasonable method of producing tricalcium phosphate appears to be reacting calcium carbonate with phosphoric acid, followed by calcining and sintering stages, depending upon the final product desired. The most acceptable pore-forming material appears to be naphthalene, which serves well as a sacrificial, void-forming element. For directional porosity formation extrusion techniques appear to be the preferred technique.

In vivo studies showing the metabolic fate of calcium from the tricalcium phosphate suggests that the calcium is freely mixed with the total body pool, and no unique or deleterious accumulations of calcium derived from the artificial material appear to be present. Further, extensive histologic analyses of various forms of the material indicate that the material is osteophilic, biocompatible, and bioresorbable. In addition to the research performed at Battelle Columbus, numerous variations of the material were supplied to the U.S. Army Institute for Dental Research, as well as other laboratories specified by the Army for various *in vivo* research protocols. These studies provided background information for the eventual commercialization of the material by independent biomaterials companies. Granular forms of the material are widely used for periodontal disease treatment. In addition clinical trials with solid material have been performed by clinical investigators independently of this program. Thus, this program is responsible for spawning a new area of biomaterials; namely, bioresorbable ceramics that can successfully serve as a scaffold for bone ingrowth.

Later studies at Battelle were aimed at increasing the strength of the bioceramic, as well as simultaneously reducing the probability of premature, deleterious bioresorption prior to adequate bone ingrowth necessary to provide adequate integrity for the area being repaired. Three various independent generations of directional porosity material were developed and subsequently evaluated. These materials by virtue of their higher density were stronger and also proved to provide greater mechanical integrity during the biodegradation process. This development was considered important since segments with omnidirectional porosity were often observed to prematurely biodegrade prior to adequate formation of osseous tissue completely through the implant. Further, the innovation allowed a wide range of biomaterials to be developed which can vary in mechanical strength and biodegradation rate, primarily based upon porosity content. It was found desirable to maintain tricalcium phosphate as a pure beta phase material, even though it is possible to vary biodegradation rate by slightly varying the stoichiometry of the material.

This directional material shows future promise for a bone ingrowth scaffold, especially in areas where low levels of stress are placed upon the implant, or where the implant can be appropriately supported by fixation. On the horizon, the use of the tricalcium phosphate matrix as a carrier for osteogenic material offers promise for rapidly forming new bone in areas where normal healing and fixation techniques are inadequate.

TABLE OF CONTENTS

	<u>Page</u>
BACKGROUND, PROBLEM, AND APPROACH	1
MATERIALS AND METHODS	3
Directional Materials Development	3
First Generation	3
Second Generation	4
Third Generation	7
Experimental Animal Studies	10
Research Protocol	10
RESULTS OF SECOND GENERATION IN VIVO EXPERIMENTS	11
Radiographic Examination of Tricalcium Phosphate	
Biodegradability	11
Histologic Evaluations	23
CONCLUSIONS AND DISCUSSION	36
REFERENCES	42

LIST OF TABLES

TABLE 1. X-RAY DIFFRACTION - RELATIVE PATTERN STRENGTH	4
TABLE 2. DENSITY RESULTS	5
TABLE 3. OPTIC EMISSION SPECTROSCOPY RESULTS	6
TABLE 4. POWDER CHARACTERIZATION	8

LIST OF FIGURES

	<u>Page</u>
FIGURE 1. RADIOGRAPH OF RABBIT D-81, 21 DAYS POST-IMPLANT	12
FIGURE 2. RADIOGRAPH OF RABBIT D-81, 3 MONTHS POST-IMPLANT	13
FIGURE 3. RADIOGRAPH OF RABBIT D-81, 6 MONTHS POST-IMPLANT	14
FIGURE 4. RADIOGRAPH OF RABBIT D-81, 9 MONTHS POST-IMPLANT	16
FIGURE 5. RADIOGRAPH OF RABBIT F-81, IMMEDIATELY POST-IMPLANT	17
FIGURE 6. RADIOGRAPH OF RABBIT F-81, 12 MONTHS POST-IMPLANT	18
FIGURE 7. RADIOGRAPH OF RABBIT I-81, 3 MONTHS POST-IMPLANT	19
FIGURE 8. RADIOGRAPH OF RABBIT I-81, 12 MONTHS POST-IMPLANT	20
FIGURE 9. RADIOGRAPH OF RABBIT I-81, 9 MONTHS POST-IMPLANT	21
FIGURE 10. THREE-MONTH POST-NECROPSY RADIOGRAPH OF EXCISED CALVARIUM FROM RABBIT G-81	22
FIGURE 11. SIX-MONTH POST-NECROPSY RADIOGRAPH OF EXCISED CALVARIUM FROM RABBIT E-81	24
FIGURE 12. NINE-MONTH POST-NECROPSY RADIOGRAPH OF EXCISED CALVARIUM FROM RABBIT D-81	25
FIGURE 13. TWELVE-MONTH POST-NECROPSY RADIOGRAPH OF EXCISED CALVARIUM FROM RABBIT F-81	26
FIGURE 14. TWELVE-MONTH POST-NECROPSY RADIOGRAPH OF EXCISED CALVARIUM FROM RABBIT N-81	27
FIGURE 15. PHOTOMICROGRAPH OF TRICALCIUM PHOSPHATE SPECIMEN WITH DIRECTED POROSITY, THREE MONTHS POST-IMPLANT (RABBIT G-81-3L)	28
FIGURE 16. PHOTOMICROGRAPH OF TRICALCIUM PHOSPHATE SPECIMEN WITH DIRECTED POROSITY, THREE MONTHS POST-IMPLANT (RABBIT B-81-5T)	30
FIGURE 17. PHOTOMICROGRAPH OF BONE INGROWTH INTO LONGITUDINAL PORE AT HIGH MAGNIFICATION, THREE MONTHS POST-IMPLANT (RABBIT B-81-5T)	31
FIGURE 18. PHOTOMICROGRAPH OF BONE INGROWTH INTO TRICALCIUM PHOSPHATE, SIX MONTHS POST-IMPLANT (RABBIT A-81-5L)	32

LIST OF FIGURES
(Continued)

	<u>Page</u>
FIGURE 19. PHOTOMICROGRAPH OF BONE INGROWTH INTO TRICALCIUM PHOSPHATE, SIX MONTHS POST-IMPLANT (RABBIT A-81-5T)	33
FIGURE 20. PHOTOMICROGRAPH OF TRICALCIUM PHOSPHATE SIX MONTHS POST-IMPLANT (RABBIT E-81-4T)	34
FIGURE 21. PHOTOMICROGRAPH OF BONE INGROWTH INTO TRICALCIUM PHOSPHATE, NINE MONTHS POST-IMPLANT (RABBIT C-81-LFC) . . .	35
FIGURE 22. PHOTOMICROGRAPH OF BONE INGROWTH INTO TRICALCIUM PHOSPHATE, TWELVE MONTHS POST-IMPLANT (RABBIT F-81-L2) . . .	37
FIGURE 23. PHOTOMICROGRAPH OF BONE INGROWTH INTO TRICALCIUM PHOSPHATE, TWELVE MONTHS POST-IMPLANT (RABBIT F-81-L2) . . .	38
FIGURE 24. PHOTOMICROGRAPH OF BONE INGROWTH INTO A CONTROL ANIMAL TWELVE MONTHS POST-SURGERY (RABBIT N-81-5L)	39

SUMMARY

This final report outlines a study to investigate bioresorbable ceramics for the management of hard tissue avulsive wounds and orofacial fractures. The study spans a long time period, and consequently, includes several innovations and changes in project direction.

The initiation portion of the study was the development and subsequent evaluation of numerous granular forms of ceramic materials that might potentially be biodegradable, osteophilic, and biocompatible. Numerous materials were prepared and implanted. The initial implant studies were performed at the U.S. Army Institutes of Dental Research. These initial studies indicated that tricalcium phosphate was a manufacturable and bioresorbable ceramic worthy of further development.

In addition to granular materials, calcium phosphates were developed in large segments. Materials ranging from fully dense to high-porosity materials were developed and evaluated in numerous animal models. Pore structure and chemical composition, as well as pore directionality, were extensively evaluated. Various manufacture methods were evaluated. The most reasonable method of producing tricalcium phosphate appears to be reacting calcium carbonate with phosphoric acid, followed by calcining and sintering stages, depending upon the final product desired. The most acceptable pore-forming material appears to be naphthalene, which serves well as a sacrificial, void-forming element. For directional porosity formation, extrusion techniques appear to be the preferred technique.

In vivo studies showing the metabolic fate of calcium from the tricalcium phosphate suggests that the calcium is freely mixed with the total body pool, and no unique or deleterious accumulations of calcium derived from the artificial material appear to be present. Further, extensive histologic analyses of various forms of the material indicate that the material is osteophilic, biocompatible, and bioresorbable. In addition to the research performed at Battelle Columbus, numerous variations of the material were supplied to the U.S. Army Institute for Dental Research, as well as other laboratories specified by the Army for various *in vivo* research protocols. These studies provided background information for the eventual commercialization of the material by independent biomaterials companies. Granular forms of the material

are widely used for periodontal disease treatment. In addition, clinical trials with solid material have been performed by clinical investigators independently of this program. Thus, this program is responsible for spawning a new area of biomaterials; namely, bioresorbable ceramics that can successfully serve as a scaffold for bone ingrowth.

Later studies at Battelle were aimed at increasing the strength of the bioceramic, as well as simultaneously reducing the probability of premature, deleterious bioresorption prior to adequate bone ingrowth necessary to provide adequate integrity for the area being repaired. Three various independent generations of directional porosity material were developed and subsequently evaluated. These materials by virtue of their higher density were stronger and also proved to provide greater mechanical integrity during the biodegradation process. This development was considered important since segments with omnidirectional porosity were often observed to prematurely biodegrade prior to adequate formation of osseous tissue completely through the implant. Further, the innovation allowed a wide range of biomaterials to be developed which can vary in mechanical strength and biodegradation rate, primarily based upon porosity content. It was found desirable to maintain tricalcium phosphate as a pure beta phase material, even though it is possible to vary biodegradation rate by slightly varying the stoichiometry of the material.

This directional material shows future promise for a bone ingrowth scaffold, especially in areas where low levels of stress are placed upon the implant, or where the implant can be appropriately supported by fixation. On the horizon, the use of the tricalcium phosphate matrix as a carrier for osteogenic material offers promise for rapidly forming new bone in areas where normal healing and fixation techniques are inadequate.

BACKGROUND, PROBLEM, AND APPROACH

Historically, various techniques have been employed for the repair or treatment of osseous diseases, defects, and wounds. Autogenous bone grafting remains the most satisfactory approach, but is not without the disadvantages associated with double surgeries, limits in structural properties, and the limitations imposed on the repair of massive osseous defects.

Since April, 1969, Battelle's Columbus Division has been conducting research under contract to the U.S. Army Institute of Dental Research (USAIDR) to develop resorbable ceramics for potential application in the repair of hard tissue avulsive wounds. The basic materials have been calcium-essential elements of the natural bone mineral phase, calcium hydroxyapatite.

In vivo studies were conducted initially at USAIDR, using the sintered porous materials and slurries prepared at Battelle from tricalcium phosphate $\text{Ca}_3(\text{PO}_4)_2$ and other calcium orthophosphate powders CaHPO_4 and $\text{Ca}(\text{H}_2\text{PO}_4)_2$, to evaluate the potential use of calcium phosphates to both facilitate repair of bone defects and to determine the best material for future exploration(1-3). The implant studies indicated that calcium phosphates consisting essentially of the mineral phases $\text{Ca}(\text{PO}_3)_2$, $\text{Ca}_3(\text{PO}_4)_2$, and CaHPO_4 are well tolerated by the tissue, appeared to be nontoxic, resorbable, and permitted rapid invasion of new bone.

Of the various porous calcium phosphate materials investigated, tricalcium phosphate, $\text{Ca}_3(\text{PO}_4)_2$, was selected for continued development and evaluation since it was easy to fabricate and was found to be both biocompatible and resorbable. Emphasis was directed toward producing porous materials consisting of single-phase tricalcium phosphate (TCP)(4-7).

Subsequent research at Battelle-Columbus was then focused on producing practical large segment replacement implants from TCP. To provide basic resorption data on the in vivo behavior of solid tricalcium phosphate bioresorbable ceramics, implants studies were initiated in 1975 at Battelle using the rabbit calvarium model(8). Early samples of tricalcium phosphate were implanted as a control and samples of two new materials were implanted for comparative observation. These new materials were prepared using improved processing techniques derived in previous materials development studies and represented significant improvements in the structural characteristics of porous tricalcium phosphate. The characterization of the materials involved and the results of

the in vivo studies were the subject of the Fifth Report(8). These results indicated that the improved material exhibited significance increases in resorption rate. In fact, the material resorbed so rapidly that after the ninth month the implant appeared to be granulated and was invaded with connective tissue. This results does not imply lack of biocompatibility, but does suggest that such rapid degradation can be deleterious in stress-bearing situations.

To determine the effects of structural variations on resorption rate, experimental porous implants were prepared using a single tricalcium phosphate powder with different pore size distribution. Three materials were prepared for in vivo evaluation. These studies demonstrated that orientation of pore structure is a more important variable than pore size distribution(9). The study indicated that a higher density material of the stoichiometric chemistry with directional porosity is probably the desired material.

The seventh report(10) demonstrated that the concept of directional porosity could provide a satisfactory result; adequate ingrowth of bone to provide mechanical integrity prior to loss of mechanical integrity of the tricalcium phosphate. These results were corroborated by Tortorelli(11). The material used in these experiments was far from ideal; consequently, a better method of production was sought. The eighth report outlines the development of a better material, the second generation material, and early phases of its in vivo evaluation(12).

The ideal material should minimally inhibit the ingrowth of bone; consequently, large pores and a high pore density are desirable. The ideal material should also be of high strength and should have mechanical properties approaching bone. Consequently, a material of high density in the non-porous regions was sought. It was also deemed desirable to have a material that could be readily manufactured with the pore alignment and size required for a particular application. A material with many of the characteristics of the ideal was developed as described in the ninth report(13) and subsequently evaluated.

MATERIALS AND METHODS

Numerous biomaterials processing techniques were utilized throughout this project to produce various forms of tricalcium phosphate. Basically, tricalcium phosphate by either reacting reagent grade basic tricalcium phosphate with phosphoric acid and water or utilizing calcium carbonate with phosphoric acid. The former method was used in the earlier studies. The early studies developed granular materials containing defined porosities of uniform size. These materials were the subject of numerous investigations at USAIDR and elsewhere. Commercial granular products are now available, based upon the discussions of this project. The subsequent sections describe the solid directional materials which represent the most sophisticated products developed. The optimum processing techniques developed for the production of tricalcium phosphates in several forms are included.

Directional Materials Development

First Generation

The first-generation directional material was produced by slowly mixing certified ACS calcium carbonate and phosphoric acid (assay 85.4 percent) in distilled water at 180°F to form a tricalcium phosphate (TCP) slurry. The slurry was air dried, then dried under vacuum at 220°F overnight to produce the tricalcium phosphate powder. This powder was then used in fabricating the directed porosity blocks. A method was found that by using a No. 8 size silk thread (~300 micron) unidirectional pores could be formed in tricalcium phosphate blocks. This procedure consisted of layering TCP powder 1/8-inch-thick in a steel die, and adding parallel rows 1/8-inch apart of wax-coated silk thread, followed by another layer of powder. This process was repeated to produce 8-layer silk thread compacts. The compacts were fired to 500°C incrementally over a five-day period to burn out the silk threads. The compacts were then sintered for two hours at 1150°C to produce a unidirectional tricalcium phosphate block.

The material manufactured by this procedure was judged adequate for proof of concept in vivo analysis. Unfortunately, the material was much weaker

than desired, the pore density was much lower than desired, and the pores were only unidirectional, and not interconnected.

Second Generation

Certified ACS calcium carbonate was combined with certified ACS phosphoric acid to form a powder precipitate by slowly mixing these two components into distilled water at 180°F. Once dried in air, the powders were dried under vacuum, 220°F, overnight. Approximately 4800 gms of material in six batches were prepared in this manner.

X-ray diffraction analysis of the above prepared powder revealed it to be hydroxyl-apatite with a trace monetite. The powder surface area was 12 m²/gm, which would mean a particle size in the submicron range. To crush the large, hard agglomerates, the hydroxy-apatite was dry ball milled for 2 hours in a polyethylene container with aluminum oxide balls. To determine the optimum calcining temperature to convert hydroxyl-apatite to whitlockite, five-100 gm samples were calcined for 3-1/2 hours at 1400, 1500, 1550, 1600, and 1700°F, followed by an X-ray diffraction analysis and a surface area test. The maximum surface area of 8.2 m²/gm and simultaneous maximum conversion to whitlockite occurred at 1550°F. Table 1 shows X-ray diffraction results at the various temperatures evaluated.

TABLE 1. X-RAY DIFFRACTION - RELATIVE PATTERN STRENGTH

Calcine Temperatures, °F	Hydroxyl- apatite	Monetite	Whitlockite	α Ca ₃ (PO ₄) ₂	Surface Area (m ² /gm)
	100	25			12.07
1400	85		100	50	11.28
1500	18		100		10.38
1550	2		100		8.2
1600	2		100		2.98

To break up agglomerates formed during calcining, the powder was ball milled with hexane for 12 hours in a polyethylene jar with aluminum oxide balls. Table 2 lists characterizations done on two powders.

TABLE 2. DENSITY RESULTS

	Calcined 1550°F	Calcined 1550°F, Then Ball Milled
Bulk density (percent theoretical)	10.6%	16%
Tap density (percent theoretical)	14.1%	23.5%
Surface area m ² /gm	8.2	11.6

To further characterize this powder, pellets were pressed and sintered at 2,000, 2050, and 2100°F. In this temperature range, tricalcium phosphate has a destructive transformation from β to α form, with the alpha form being of lower density. The highest sintered density was obtained by heating to 2050°F in 1 hour, holding for 2 hours, and cooling slowly (overnight) to room temperature. This yielded a sintered pellet with 92 percent theoretical density and a linear shrinkage of 12 percent.

An alumina powder, A-16SG, made by Alcoa, was chosen for preliminary binder studies since its particle size distribution and surface area, 10-12 m²/gm is similar to the tricalcium phosphate material being used. Various compositions containing A-16SG alumina, an organic solvent, binder, plasticizer, and a deflocculant were mixed, milled for 24 hours, and cast. Once a suitable composition--one which dried easily without cracks and had excellent flexibility--was found, the tricalcium phosphate material was used in place of the A-16SG alumina. The composition was a polymeric formulation containing appropriate dispersing agents.

An embossing tool was machined from a Teflon rod with circular grooves of the dimensions required. During the drying of the tricalcium phosphate tape cast piece, the embossing tool was rolled over the surface, producing

the grooves. After the fluted sheets dried in ambient conditions for 15 to 30 minutes, 3/4-inch squares were cut from the sheets by using a razor knife. An Exacto saw was used to cut small interconnecting channels through the embossed ribs perpendicular to the main channels. The ceramic-organic slurry was painted on the underside of the tricalcium phosphate square, and the squares were stacked in alternate directions at right angles. Finally, a 20-gauge drill was used to produce a connecting hole between layers of the matrix.

Removal of the organic binders and the sintering of the matrix structure was accomplished in one step. The embossed tape cast pieces were heated in 1 hour to 2050°F and held there for 2 hours, producing pieces with a density of ~50 percent of theoretical. The organic binders were removed from the pieces without producing cracks. Because of the destructive nature of the α to β transformation, the sintering temperature was 2000°F, resulting in a 100 percent β tricalcium phosphate. This method should result in higher strength with little or no reduction in density. These segments were subsequently cut into circular segments for *in vivo* analysis.

To characterize the matrix structure, X-ray diffraction, optical emission spectroscopy, and fired density measurements were conducted. X-ray diffraction analysis proved the matrix structure to be 100 percent β tricalcium phosphate. Optical emission spectroscopy results are listed in Table 3.

TABLE 3. OPTIC EMISSION SPECTROSCOPY RESULTS

Element	Weight Percent as Metal
Ba	T
B	T
Si	0.01
Fe	T
Mg	T
Al	0.05
Mo	T
Cu	T
W	0.02
Na	0.02
Li	T
Sr	0.03

Mercury displacement showed that the fired density of the matrix was 57.3 percent of theoretical, and the fired density of the laminated implant structure was approximately 35 percent of theoretical.

Although the overall (bulk) density of the material was lower than the previous random porosity implant materials (48-52 percent), the material appeared to have a higher transverse strength. However, there was a tendency to delaminate between layers because of incomplete bonding. Processing improvements were needed to increase strength and achieve better bonding. An increase in bulk density back to the 50 percent range may be necessary to achieve these improvements. This will necessitate developing tape compositions having higher loading of TCP or the adoption of alternative processes.

Third Generation

The final materials development for this project was the development of a third generation directional porosity material with improved mechanical properties. Several methods for the material were proposed. However, the hot extrusion forming was the method selected for extensive development and evaluation. The ceramic preparation was performed in a series of tasks and is discussed in the following paragraphs.

Calcium carbonate was combined with phosphoric acid to form a powder precipitate by slowly mixing these two components at 180°F. Once dried in air, the powders were dried under vacuum, 220°F, overnight. Approximately 6.4 kg of material in eight batches were prepared in this manner.

X-ray diffraction analysis of the above powder revealed it to be hydroxyi-apatite with a trace of monolite. The powder surface area was 13.6 m²/gm, which would indicate a mean particle size in the submicron range. To crush the large, hard agglomerates, formed during drying, the precipitate powder was dry ball milled for 2 hours in a polyethylene container with aluminum oxide balls. To convert the hydroxyl-apatite to whitlockite, the powder was calcined for 3-1/2 hours at 1500°F followed by an X-ray diffraction analysis. The powder was 100 percent converted to whitlockite. To break up sintered agglomerates, the calcined powder was ball milled with hexane for 12 hours in a polyethylene jar with aluminum oxide balls. The following characterization was performed on the powder.

TABLE 4. POWDER CHARACTERIZATION

	As Produced	Ball Milled 2 Hours	Calcined at 1550°F Hexane Ball Milled
Bulk density percent theoretical	10.3	17.4	23.1
Tap density percent theoretical	15.0	27.8	36.8
Surface area m^2/gm	13.57	16.4	TBD

Since the characteristics of this powder are similar to those of powders previously produced, a sintering study of this powder was not undertaken. As previously mentioned, the sintering temperature of the tricalcium phosphate matrix was at 2000°F to avoid the destructive β to α conversion.

When formulating mixes for hot extrusion or injection molding, one attempts to obtain the optimum binder content for molding. This optimum is a condition that represents a balance between maintaining the rheological condition for molding and a minimum amount of binder.

A practical method has been found for determining an optimum binder concentration for a given powder without making an elaborate characterization of the powder. The method is a modification of the ASTM D-281-31 oil adsorption test. The modification consists of the use of the Brabender Plastograph to minimize the operator variance factor.

In this method, the powder is mixed with an oil, the oil being added at a constant rate while the torque is recorded by the plastograph. The point at which the maximum torque occurs is interpreted as being the critical powder volume concentration (CPVC).

Expressed as an equation, CPVC becomes:

$$CPVC = \frac{\text{Volume of Powder}}{(\text{Volume of Powder} + \text{Volume of Oil})}$$

For tricalcium phosphate, the CPVC equalled 64.0 percent. Converting from a volume percentage to a weight percent, this optimum binder concentration is 14 weight percent organic and 86 weight percent tricalcium phosphate. From this, a ceramic-organic mix was formulated containing a plasticizer, a wax, and a surfactant, having a combined weight of 14 percent of the batch.

The previously employed tape casting process contained 20.7 weight percent organic binder. This 6.7 weight percent reduction organic content, along with an improved forming technique, has resulted in improved sintered densities.

To obtain sheets of correct thickness, a die was purchased from Brabender Plastograph Company having the capability of extruding sheets ranging in thickness from 1.5 to 3.0 mm with a predetermined width of 25 mm. Using the mix formulated as described above, flat sheets 25 mm wide and 1.5 mm thick were formed by hot extrusion. An embossing tool was machined from a Teflon rod with circular grooves of the dimension required. After extrusion, the sheets are heated and embossed.

A second requirement of the matrix structure was the presence of vertical passages between layers. Several mechanical methods, drilling, punching, etc., were examined using the embossed sheets prior to stacking or burnout. However, in most cases, these techniques resulted in severe cracking. An alternative method investigated was laser drilling. Single embossed sheets were quickly laser drilled by a Neodymium glass pulse laser.

Efforts were focused on the prevention of delamination, which was a problem identified earlier in the program. The objective has been to minimize or eliminate the problem by enhancing the physical bonding of tricalcium phosphate particles from neighboring layers. Simply stacking the sheets prior to binder burnout is not adequate. After several experiments, the best enhancement of the interlayer bonding was achieved by coating the surface of the embossed sheet with an oil or solvent followed by stacking, burnout, and sintering.

Removal of the organic binder from the matrix structure was accomplished using a 10-day burnout cycle with a heating rate of 2°C per hour. Faster heating rates resulted in collapse of the structure as a consequence of melting of the binder before sufficient sublimation had occurred to produce a rigid structure.

After burnout, the matrix structure was heated in 1 hour to 2000°F and held at temperature for 2 hours, producing a structure with a sintered matrix density of 82 percent of theoretical. This was an outstanding improvement over the tape cast sheets which has sintered densities below 50 percent of theoretical.

Experimental Animal Studies

This portion of the report details the various research procedures which were used in our laboratories to evaluate the biodegradable materials.

Research Protocol

In order to test the biodegradation of large tricalcium phosphate segments, a special experimental model was devised. These basic methods were employed to evaluate several variations of unidirectional and omnidirectional tricalcium phosphate. The mature, male, New Zealand white rabbit was used. The calvarium was found to be an excellent test implant site for this biomaterial. Since stresses upon the calvarium are not extraordinarily high, external stabilization is not required. Consequently, confusing effects which might be due to stabilization devices were not seen. Of greater importance is the fact that this implant site provided a large, relatively uniform area for various simultaneous studies such as periodic radiography, multiple histologic analyses, etc.

Standard aseptic surgical technique was used to expose the calvarium of the anesthetized animal. A circular, 8 mm diameter, portion of the calvarium or optionally a rectangular segment was osteotomized bilaterally with no attempt to salvage the periosteum overlying the excised area. The tricalcium phosphate implants were interference fit. The skin incision was closed and the animal was treated with a prophylactic antibiotic.

For the second-generation, directional materials in vivo results, 14 animals were randomly separated into four experimental groups. The experimental groups consisted of sacrifice dates 3, 6, 9, and 12 months post-implant. Since two implants were placed in each animal, four samples were available for analysis at each sacrifice interval. Two control animals were prepared.

These animals had bilateral circular voids 8 mm in diameter. The animals were radiographed at 3-month intervals until the time of necropsy. Excised skulls were radiographed post-necropsy. In addition, implants were radiographed prior to surgery. A step wedge was incorporated into all radiographs to facilitate comparisons.

Histologic technique consisted of embedding portions of the excised calvarium-tricalcium phosphate complex in methylmethacrylate and sectioning. Half of each excised sample was stained with basic fuchsin prior to sectioning. During the experiment, rabbits were stained at time zero and 3-month intervals with one of the following vital bone growth markers: tetracycline, 60 mg/kg; DCAF, 20 mg/kg; and xylenol orange, 90 mg/kg. The other half of the above-mentioned sample was left unstained and sectioned for ultraviolet bone growth analysis utilizing these previous injected vital bone growth markers.

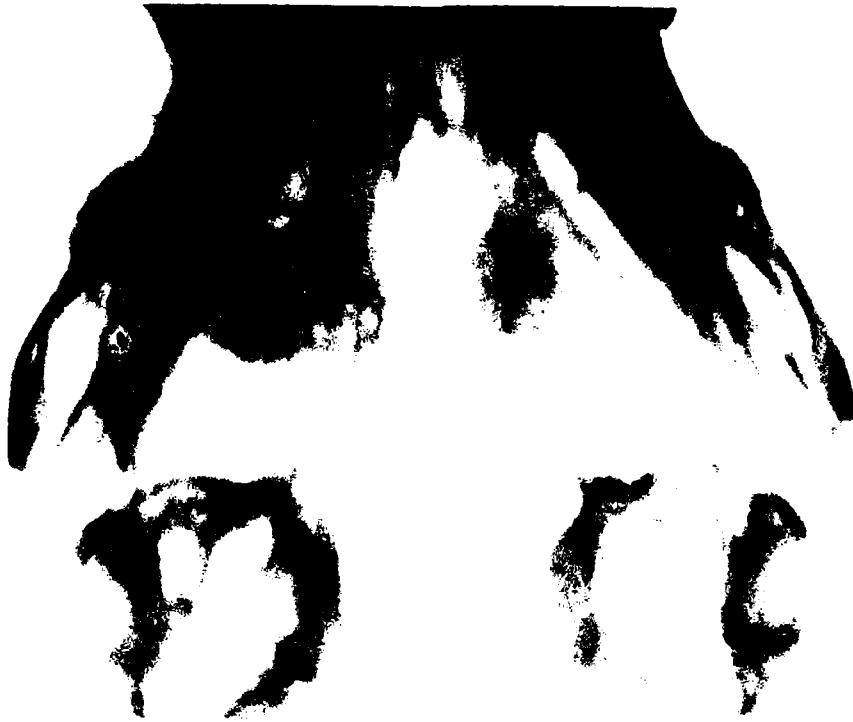
RESULTS OF SECOND GENERATION IN VIVO EXPERIMENTS

Radiographic Examination of Tricalcium Phosphate Biodegradability

Representative of the results are the radiographs of rabbit D-81. Figure 1 shows in situ tricalcium phosphate implants 21 days post-implant. Note that the implants are readily apparent in the animals' calvarium. In this "live" X-ray, detail of the directed porosity of the implant is not distinct. The radiodensity of both implants appears equivalent.

Figure 2 is a radiograph of the same animal (D-81) 3 months post-implant. The overall radiodensity of the implants is lower, suggesting some bioresorption within the samples. The right implant is somewhat obscured by the angle of this radiograph.

By 6 months, there was a dramatic alteration in the appearance of the samples. Figure 3 illustrates the 6-month radiograph of rabbit D-81. The samples are difficult to locate in the radiograph. This suggests that the radiodensity of the samples is approaching that of the surrounding bone and further suggests additional bioresorption.



≈ 2.5X

FIGURE 1. RADIOGRAPH OF RABBIT D-81, 21 DAYS POST-IMPLANT

The implants are readily apparent in the animal's calvarium, shown as circular images. In this "live" X-ray, the directed porosity of the implants is not readily apparent.

Note that all radiographs in this research report were exposed with a step wedge included. The step wedge was used as a control to correct for any exposure differences. Consequently, all photographs of radiographs in this report are corrected, relative to a control density.



≈2.5X

FIGURE 2. RADIOGRAPH OF RABBIT D-81, 3 MONTHS POST-IMPLANT

This radiograph shows a decrease in overall radiodensity when compared to the previous figure. This suggests some bioresorptive activity of the implanted samples.



FIGURE 3. RADIOGRAPH OF RABBIT D-81, 6 MONTHS POST-IMPLANT

This figure demonstrates a dramatic decrease in the radio-density of these samples when compared to the previous two figures. This suggests progressive bioresorption. The density of the biomaterial now approximates that of the surrounding bone.

Figure 4 is the 9-month radiograph of rabbit D-81. Only under close scrutiny can remnants of the samples be found. Again, the radiograph suggests continuing resorption of the samples.

Another example of radiodensity alteration with time can be seen in a 12-month experimental animal. Figure 5 (Rabbit F) shows an X-ray taken at "zero time". The left implant is clearly visible, but unfortunately the right implant is not clear. At 12 months (Figure 6), there is a definite decrease in density seen in the left implant. The right-hand implant is not visible. Another example of 12-month radiodensity change can be seen in Rabbit I. At three months (Figure 7) both implants are clearly visible. At 12 months (Figure 8), a definite alteration in radiodensity is seen in both samples. However, there appears to be a radiolucent area posterior to the right-hand implant. Also there appears to have been more resorption in the right implant than the left. It should be noted that the right implant was thinner than the left at the time of implant. It is further apparent that there is some inconsistency between animals in the degree of bioresorption which has taken place. Subjectively, it appears that resorption is slowing down at about month 9. For example, in Figure 9 (Rabbit I) at 9 months it is difficult to distinguish between this 9-month radiograph (left-hand implant) and the same implant at 12 months (Figure 8). This observation is opposite to the expected result. One would anticipate an increase in resorption rate with time, due to an increase in the surface area-to-volume ratios.

A better view of bioresorption can be obtained from excised skulls. Since sequential radiographs of the same animal cannot be obtained, serial necropsies at radiograph 3-month intervals are presented here. Each implant is presented directly above a pre-implant radiography of the identical specimen. This method provides an evaluation of resorption rate for the time period noted.

Figure 10 illustrates a 3-month necropsy radiograph of an excised skull (Rabbit G-81). The samples can be clearly observed in this radiograph because interfering bone and tissue structures have been removed. The same implants are illustrated below as they appeared when radiographed prior to surgery. Upon comparison, some resorption of the implants and ingrowth can be noted by widening of the directed pores and the appearance of granular material (presumably bone) within the pores. Granular-appearing material is especially noticeable in the left implant.



≈ 2.5X

FIGURE 4. RADIOGRAPH OF RABBIT D-81, 9 MONTHS POST-IMPLANT

In this figure, bioresorption is apparently extensive, remnants of the samples can be found only under close scrutiny. This is the same animal illustrated in the preceding three figures.



≈ 2.5X

FIGURE 5. RADIOGRAPH OF RABBIT F-81,
IMMEDIATELY POST-IMPLANT

This figure presents another example of directed porosity implants shortly after surgery.



≈ 2.5X

FIGURE 6. RADIOGRAPH OF RABBIT F-81, 12 MONTHS POST-IMPLANT

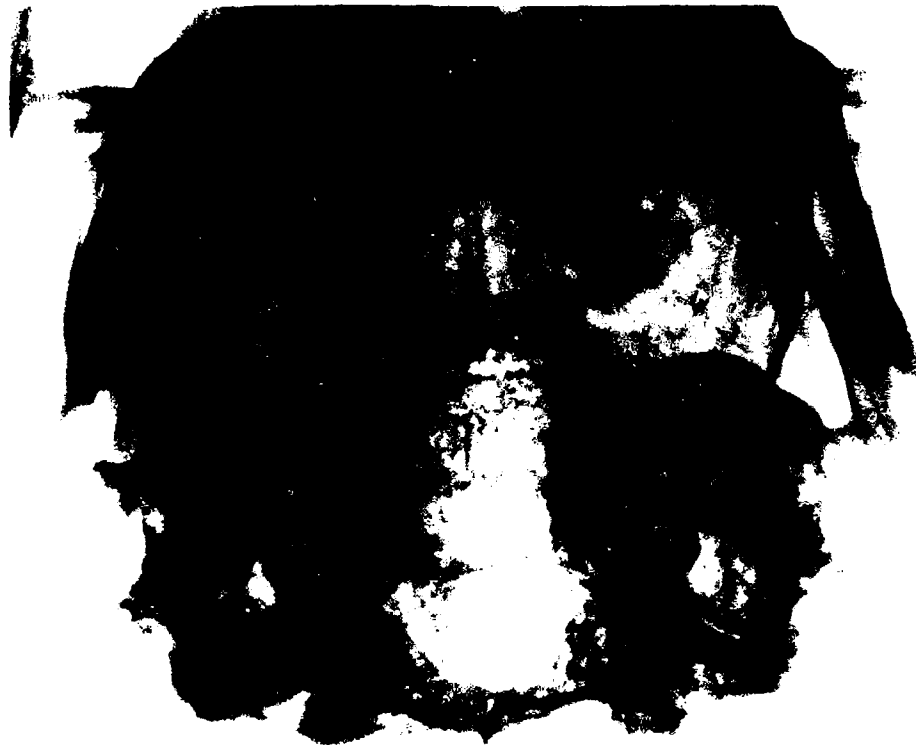
When compared to Figure 5, the radiodensity has decreased dramatically as the previous example. In this figure, there appears to be preferential resorption in the right implant and along the directed pores. The pore diameters appear to be increasing.



≈ 2.5X

FIGURE 7. RADIOGRAPH OF RABBIT I-81, 3 MONTHS POST-IMPLANT

At this time, both samples are clearly visible.



≈ 2.5X

FIGURE 8. RADIOGRAPH OF RABBIT I-81, 12 MONTHS POST-IMPLANT

When compared to Figure 7, there has been a definite decrease in the apparent radiodensity of the tricalcium phosphate implants. Further there appears to be a radiolucent area posterior to the right hand implant.



≈ 2.5X

FIGURE 9. RADIOGRAPH OF RABBIT I-81, 9 MONTHS POST-IMPLANT

In this particular animal it is difficult to distinguish between this radiograph and that taken 3 months later. Subjectively resorption appears to have slowed. This is not consistently observed in all experiments.



A



B

 $\approx 2.5X$

FIGURE 10. THREE-MONTH POST-NECROPSY RADIOGRAPH OF EXCISED CALVARIUM FROM RABBIT G-81

In Panel A, the large directed porosity of the samples are clearly visible because the interfering bone and tissue structures have been removed. In Panel B, a radiograph of the same implants prior to surgery is presented for comparison. The identical implants are located directly above. However, the implants were rotated at surgery.

The comparison of the two radiographs shows resorption as evidenced by widening and decreased radiodensity especially along the pores, and apparent ingrowth as evidenced by granular material within the pores.

Figure 11 illustrates a 6-month necropsy radiograph (Rabbit E-81). Again, a radiograph of the same samples prior to implant is included below for comparative purposes. When compared to the pre-surgery radiograph, considerable resorption of the sample and ingrowth of bone is suggested. The degree of resorption can be readily noted in the holes normal to the film plane. Their diameter has markedly increased in the six-month experimental period.

Figure 12 represents a 9-month necropsy radiograph (Rabbit D-81). Note that very significant bioresorption and bone ingrowth appears to have taken place. The change in these samples is especially dramatic when they are compared to either their control radiographs or those examples of 3- and 6-month animals. It is significant to note that there has been no loss of bone integrity. Loss of bone integrity or bone resorption when it occurs is usually noted by the radiographic appearance of large radiolucent areas.

Figure 13 represents a 12-month necropsy radiograph (Rabbit F-81). Here an impressive degree of bioresorption can be noted in both samples. The result is *much more obvious in the right-hand sample*. This sample was thinner than the left sample at the time of implant. However, even the thicker left-hand sample shows an impressive degree of internal resorption.

Figure 14 is a 12-month necropsy radiograph of a control animal (Rabbit N-81) in which holes were cut but no samples placed. This control animal clearly illustrates that a defect of this size and type will not naturally heal.

Histologic Evaluations

To evaluate the rate of ingrowth of biologic material (bone and connective tissue) into the tricalcium phosphate and the subsequent biodegradation of tricalcium phosphate, ground sections of the excised skulls were prepared. A methylmethacrylate embedding technique was used. Due to the nature of tricalcium phosphate, ground sections cannot be prepared without embedding in a rigid fixation medium such as methylmethacrylate. Sections were prepared both pre-stained with basic fuchsin and also unstained.

Figure 15 is a photomicrograph of a specimen implanted for 3 months (Rabbit G-81-3L). Both transverse and longitudinal pores can be seen. Rather extensive bone formation is seen in the lower longitudinal pore. However,



A



B

 $\approx 2.5X$

FIGURE 11. SIX-MONTH POST-NECROPSY RADIOGRAPH OF EXCISED CALVARIUM FROM RABBIT E-81

In Panel A, the samples are shown in the excised calvarium at six months post-implant.

In Panel B, the same samples are shown prior to surgery. As in the previous example (Figure 10), bioresorption and bone ingrowth appears to be under way. Resorption appears more advanced than at 3 months.



A



B

~2.5X

FIGURE 12. NINE-MONTH POST-NECROPSY RADIOGRAPH OF EXCISED CALVARIUM FROM RABBIT D-81

In Panel A, the samples are shown as they appear nine-months post-implant. In Panel B, the same implants are shown as they appeared prior to surgery.

In this figure, the apparent bioresorption and bone ingrowth is dramatic when compared to control, or to the 3- and 6-month samples (Figures 10 and 11). It is significant to note that there has been no bone loss.



A



B

 $\approx 2.5X$

FIGURE 13. TWELVE-MONTH POST-NECROPSY RADIOGRAPH OF EXCISED CALVARIUM FROM RABBIT F-81

In Panel A, the samples are shown as they appear 12 months post implant. In Panel B, the same implants are shown as they appeared prior to surgery. Extensive resorption is seen in both samples. However, resorption is much more complete on the right, where a somewhat thinner implant was used.



≈2.5X

FIGURE 14. TWELVE-MONTH POST-NECROPSY RADIOGRAPH OF
EXCISED CALVARIUM FROM RABBIT N-81

This radiograph is from a control animal. The results indicate that a void of this size in the rabbit calvarium will not heal naturally.



≈ 37X

FIGURE 15. PHOTOMICROGRAPH OF TRICALCIUM PHOSPHATE SPECIMEN WITH DIRECTED POROSITY, THREE MONTHS POST-IMPLANT (RABBIT G-81-3L)

This figure shows one longitudinal pore in the lower portion of the figure with bone ingrowth. The upper longitudinal pore is filled with connective tissue. The transverse pores, seen in the middle of the figure appear as scalloped shapes. These pores are at right angles to the pore layers above and below. These pores contain bone, some connective tissue and marrow-filled spaces similar to those normally seen in the diploë of rabbit calvaria.

Note: Included in the rabbit identification, is the slide number from which the particular photomicrograph was obtained. For example, in this figure, -3L identifies the slide number.

mostly dense connective tissue fills the upper longitudinal pore. Between the two longitudinal pores are the scalloped shapes produced by transverse pores which are extending at right angles to the plane of the figure. These pores are filled with bone, some connective tissue, and diplöe-like spaces, which apparently contain marrow.

Figure 16 is a photomicrograph from another three-month animal (Rabbit B-81-5T). This figure presents a somewhat different appearance than the previous figure. In a longitudinal pore (shown at the bottom of the figure) bone appears to be closely adapted to the tricalcium phosphate wall of the pore, whereas the central portion of the pore appears to contain voids similar to those normally seen in the diplöe layer of calvarium bone. The diplöe is generally trabecular-like bone with marrow filling most of the void spaces. The old bone is at the left and bone ingrowth appears to be proceeding into the large pores. Bone within the biomaterial appears similar in morphology to the old bone.

Figure 17 is a higher magnification of the same area (Rabbit B-81-5T). Note the close adaptation of bone to the tricalcium phosphate. Osteoblast-like cells appear to be lined up at the bone-biomaterial interface.

Figure 18 is a photomicrograph from a 6-month experiment (Rabbit A-81-5L). All available pore spaces appear to be packed with bone or diplöe-like spaces filled with marrow. Generally, bone occupies all the available biomaterial interface space. Figure 19 is a photomicrograph of the contralateral tricalcium phosphate implant (Rabbit A-81-5T). Again, bone and diplöe marrow spaces are seen filling the available biomaterial pore space. However, in this sample it appears that considerably more bioresorption has taken place as evidenced by the thin spicules of tricalcium phosphate that remain.

Figure 20 is a higher magnification photomicrograph from a 6-month implant specimen (Rabbit E-81-4T). In this case, a transverse pore is shown. As noted previously, bone appears to adapt closely to the biomaterial whereas the central portion of the pore is filled with a non-osseous, diplöe-like space filled with marrow.

Figure 21 is a photomicrograph from a 9-month specimen (Rabbit C-81-LFC). This particular section is unusual in that the degree of bioresorption is extreme, as compared to 12-month samples. This example indicates that variability was observed, in terms of inter-specimen resorption rate.



≈ 37X

FIGURE 16. PHOTOMICROGRAPH OF TRICALCIUM PHOSPHATE SPECIMEN WITH DIRECTED POROSITY, THREE MONTHS POST-IMPLANT (RABBIT B-81-5T)

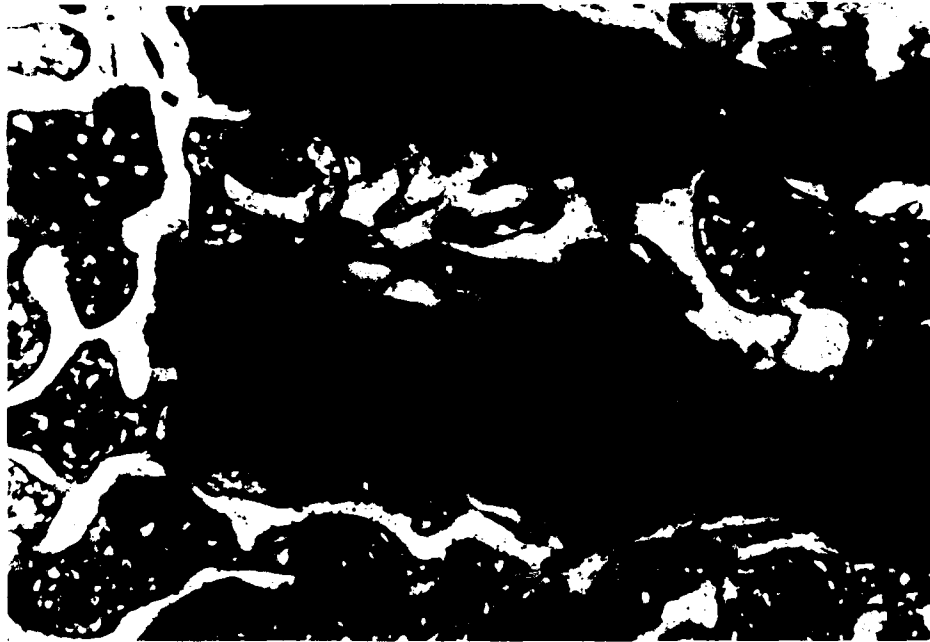
This implant exhibits bone ingrowth preferentially at the bone biomaterial interface. The longitudinal pore at the bottom of the figure shows bone closely adapted to the tricalcium phosphate. The center of the pore contains marrow space. The bone appears to have grown from the old bone, at the left, unimpeded by the presence of the biomaterial.



≈ 90X

FIGURE 17. PHOTOMICROGRAPH OF BONE INGROWTH INTO LONGITUDINAL PORE AT HIGH MAGNIFICATION, THREE MONTHS POST-IMPLANT (RABBIT B-81-5T)

This view shows the close adaptation between bone and tricalcium phosphate. There does not appear to be a continuous connective tissue layer at this interface. Osteoblast-like cells appear lined up at the bone-biomaterial interface.



≈37X

FIGURE 18. PHOTOMICROGRAPH OF BONE INGROWTH INTO TRICALCIUM PHOSPHATE, SIX MONTHS POST-IMPLANT (RABBIT A-81-5L)

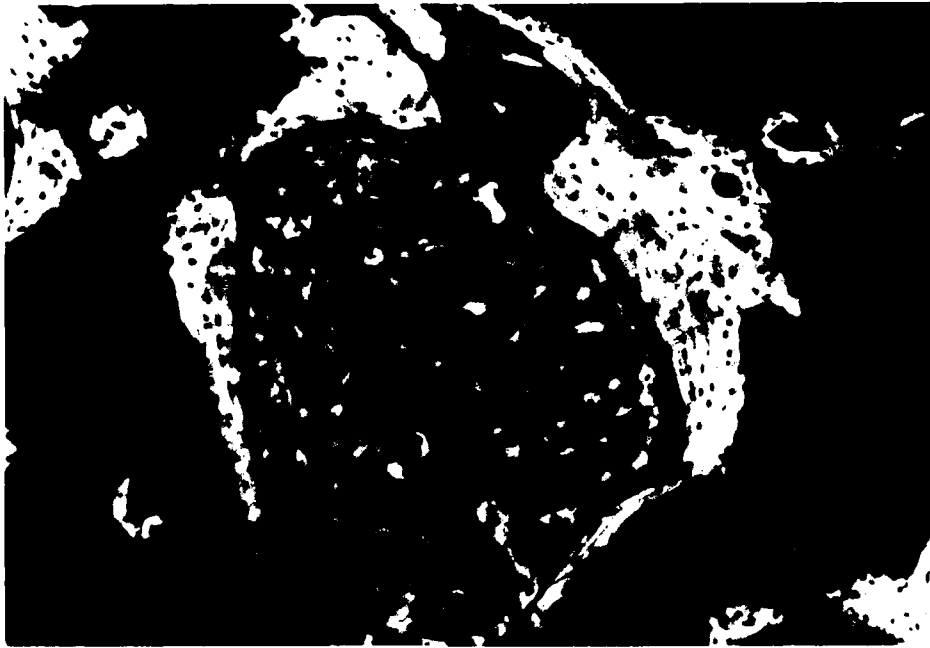
At six months, all available spaces within the implant appear densely packed with bone and marrow spaces. As seen previously bone is predominantly seen at the biomaterial interface.



≈ 37X

FIGURE 19. PHOTOMICROGRAPH OF BONE INGROWTH INTO TRICALCIUM PHOSPHATE, SIX MONTHS POST-IMPLANT (RABBIT A-81-5T)

This figure demonstrates extensive bioresorption of the tricalcium phosphate. The walls of biomaterial between the pores have been reduced to spicules. As in previous figures all available space is packed with bone and/or marrow space. The consistency of the bone approximates that of normal calvarium.



≈ 90X

FIGURE 20. PHOTOMICROGRAPH OF TRICALCIUM PHOSPHATE SIX MONTHS POST-IMPLANT (RABBIT E-81-4T)

This figure at high magnification shows the close adaptation of bone to the biomaterial. The periphery of the pore contains dense bone, whereas the central pore area contains marrow space.



≈ 37X

FIGURE 21. PHOTOMICROGRAPH OF BONE INGROWTH INTO TRICALCIUM PHOSPHATE, NINE MONTHS POST-IMPLANT (RABBIT C-81-LFC)

This unstained specimen demonstrates extensive bioresorption of the tricalcium phosphate.

This particular 9 month implant underwent more resorption and subsequent bone replacement than most comparable samples. It is significant that mechanical integrity was not lost, even with the extreme example of resorption.

This particular unstained section does not show good bone detail. However, the pattern is consistent with the previously presented photomicrograph: bone close adapted to the tricalcium phosphate with open diplöe-appearing spaces. Blood-formed elements are not visible in this preparation.

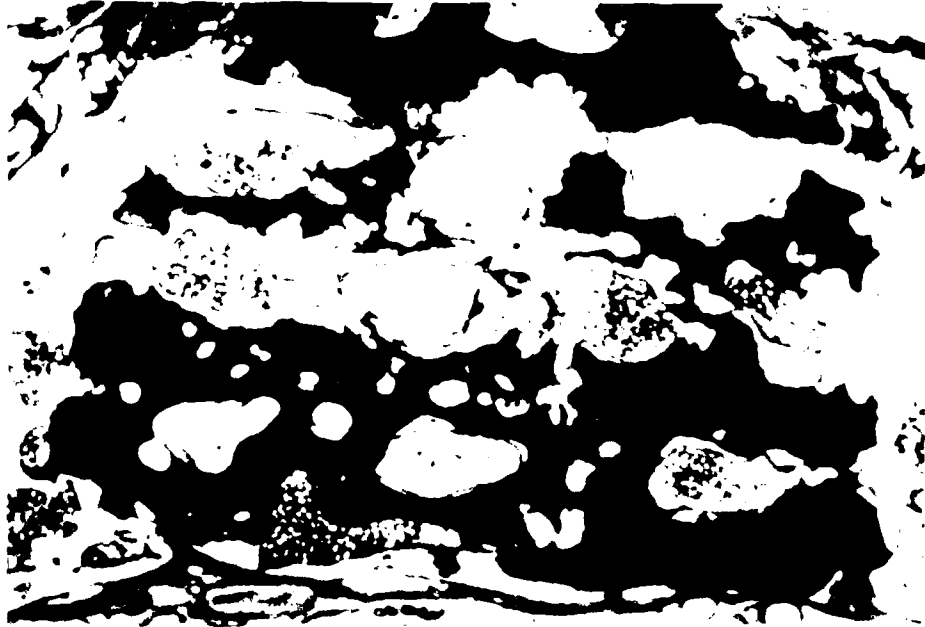
Figure 22 illustrates a 12-month photomicrograph (Rabbit F-81-L2). The resorption process is not as obvious as the previous 9-month example. However, the internal structure of the implant is well on its way to being replaced with bone. It is significant to note that mechanical integrity of the implant or surrounding bone was not lost in this animal or any of the experimental animals.

Figure 23 is a high magnification photomicrograph of a 12-month animal (Rabbit F-81-L2). Again the consistent pattern of close adaptation of bone to the tricalcium phosphate is present. The bone structure again has typical diplöe-like spaces. This area of the implant appears to contain a higher percentage of bone than implant, thus indicating significant resorption. The two previous photomicrographs are from the left-hand sample from Rabbit F, as shown in the radiographs of that animal. Figure 24 is a photomicrograph of a 12-month control animal which was not implanted (Rabbit N-81-L1). Note that the void area is bridged by connective tissue, and bone formation has occurred only at the periphery of the void. This figure illustrates that the size of void used will not naturally be repaired by bone ingrowth.

CONCLUSIONS AND DISCUSSION

This study indicates that the use of longitudinally organized unidirectional implant pores is a viable method to prevent the deleterious loss of implant and bone integrity. Such loss of integrity was seen in previous experiments when omnidirectional materials were studied.

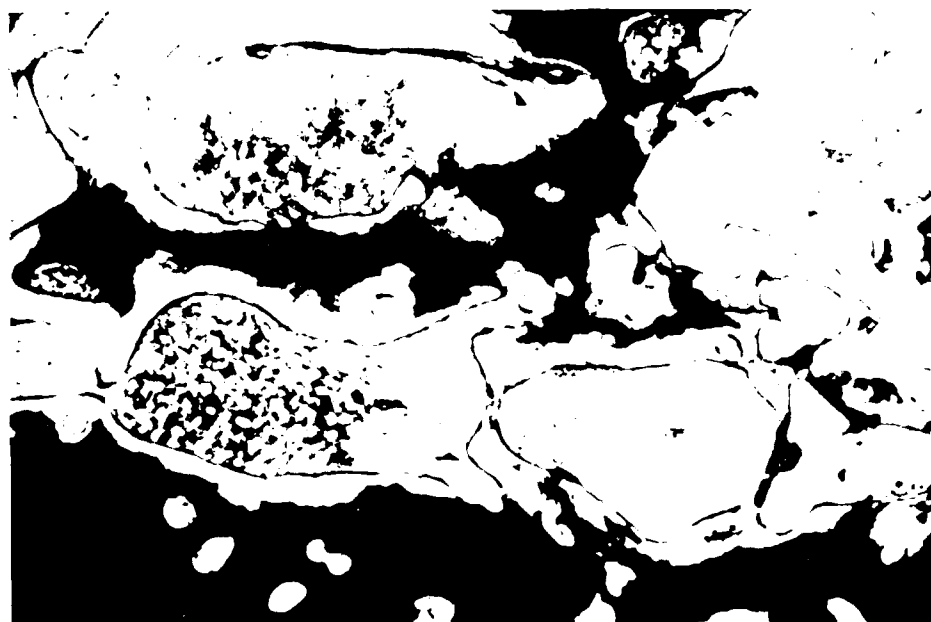
Integrity has continually plagued the use of omnidirectional structural bioresorbable bone scaffold materials. The omnidirectional design has two major drawbacks. First, the initial strength of the material is severely limited. Second, and more importantly, as bone grows in and the material simultaneously biodegrades, mechanical integrity of the biomaterial-bone complex may be lost. The result is a bone loss and filling of the area with connective



≈37X

FIGURE 22. PHOTOMICROGRAPH OF BONE INGROWTH INTO TRICALCIUM PHOSPHATE, TWELVE MONTHS POST-IMPLANT (RABBIT F-81-L2)

This figure demonstrates less extensive bioresorption of tricalcium phosphate than seen in the previous 9 month example (Figure 21). Some 12 month specimens exhibit more extensive resorption for example, Figure 13.



≈ 90X

FIGURE 23. PHOTOMICROGRAPH OF BONE INGROWTH INTO TRICALCIUM PHOSPHATE, TWELVE MONTHS POST-IMPLANT (RABBIT F-81-L2)

This figure demonstrates extensive bioresorption of the tricalcium phosphate histologically consistent having an appearance consistent with other specimens observed at high magnification.



≈37X

FIGURE 24. PHOTOMICROGRAPH OF BONE INGROWTH INTO A CONTROL ANIMAL TWELVE MONTHS POST-SURGERY (RABBIT N-81-5L)

This figure demonstrates that bone ingrowth will not naturally occur into the void used in this experiment.

connective tissue in response to loss of stability. With the unidirectional material presented in this report, the use of relatively large channels for bone to grow through, coupled with a stronger wall material, appears to provide adequate mechanical integrity during the resorption process to prevent bone loss.

This report provides animal data up to 12 months post-implant on material termed "second generation". This material had relatively large and directional pores of approximately 450 microns. The pores were running at 90° alternating direction every layer. This material suffered from low mechanical strength at the interfaces of the sheet laminates used to construct the composite. It also had less than the desired distribution of cross connections. Despite these problems the material had vastly improved bulk strength properties as compared to omnidirectional and first generation unidirectional materials. The improved strength opens up numerous additional possibilities for the potential application of the material. An obvious advantage is that less external fixation will be required when this material is utilized. The material will also be able to accommodate more loading during the bone ingrowth, remodeling, and implant resorption.

The most important finding of this study is the extensive biodegeneration of the unidirectional tricalcium phosphate scaffold material without loss of the ingrowing and remodeling bone. At 12 months, there is still residual material. Consequently, the ultimate fate of this material has yet to be determined.

Inconsistency of resorption rate was noted, especially between 9 and 12 months. Some 9-month samples appeared to have proceeded as far as similar samples at 12 months. The most probable explanation for this difference is biological variability. It should also be noted that in an attempt to match the rabbit skull thickness, different thicknesses of implant were used. Since the material is of "layered" construction, removing a small amount of material will potentially uncover a whole layer of pores. In such a fashion the surface area-to-volume ratio may be dramatically altered. This is one difficulty with the present calvarium model when a relatively thick material is placed in a thin skull.

To minimize interpretation difficulties, the samples were radiographed before surgery at their actual implant thickness. Thus, by comparison to the

pre-implant radiograph, a true evaluation of resorption of any particular sample can be obtained.

The final material development aspect of this project has produced further improvements in the material. This material was termed "third generation". Unidirectional tricalcium phosphate was improved in two aspects: The interlayer bonding problem was minimized and the strength of the material was increased.

The third generation material produced in this study was tested in New Zealand white rabbits at the U.S. Army Institute of Dental Research by Dr. Jeffrey Hollinger(14). The study utilized a rabbit calvaria model with a single large disk (15 mm of tricalcium phosphate placed in the calvarium, as opposed to the studies in this report where bilateral disks were placed). Good bone ingrowth was obtained into unidirectional biomaterials as well as reference omnidirectional biomaterial samples. It appeared in this study that the unidirectional material was biodegrading at a rate slower than that observed in the studies previously performed at Battelle. This difference is possibly due to the increased density of the third generation material. In addition, the omnidirectional reference materials did not prematurely biodegrade as had been previously reported in earlier Battelle studies(8). The difference in results for omnidirectional reference material experiments cannot easily be reconciled.

These studies developed a wide variety of tricalcium phosphate biomaterials which were successfully demonstrated to serve as ingrowth scaffolds for bone matrix formation. The material has been shown to be biocompatible and osteophilic and will bone to grow in areas where it would not naturally be formed. Utility has been well demonstrated in both animal and clinical studies. The material's strength has been modified to the extremes. The material is efficacious for use as a temporary matrix, but due to its low inherent mechanical integrity and its biodegradability, cannot perform as a permanent prosthesis. However, this material does offer the potential of providing for the optimal biomaterial to be formed and that is de novo bone. Further improvements in this process will most likely come from the incorporation of a bone growth substance.

REFERENCES

- (1) Bhaskar, S. N., Cutright, D. E., Knapp, M. J., Beasley, J. D., and Perez, B. 1971. Tissue reactions to intrabone ceramic implants. Oral Surg., Oral Med., Oral Path., 31: 282-289.
- (2) Bhaskar, S. N., Brady, J. M., Getter, L., Grower, M. F., and Driskell, T. D. 1971. Biodegradable ceramic implants in bone (electronic and light microscopic analysis). Oral Surg., Oral Med., Oral Path., 32: 336-346.
- (3) Getter, L., Bhaskar, S. N., Cutright, D. E., Bienvenido, P., Brady, J. M., Driskell, T. D., O'Hara, M. J. 1972. Three biodegradable calcium phosphate slurry implants in bone. J. of Oral Surgery, 30: 263-268.
- (4) Driskell, T. D., O'Hara, M. J., and Green, G. W., Jr., D.D.S. 1971. Management of hard tissue avulsive wounds and management of orofacial fractures. Report No. 1, Contract No. DADA17-69-C-9118 (February).
- (5) Driskell, T. D., O'Hara, M. J., and Grode, G. A. 1971. Management of hard tissue avulsive wounds and management of orofacial fractures. Report No. 2, Contract No. DADA17-69-C-9118 (October).
- (6) Driskell, T. D., O'Hara, M. J., Niesz, D. E., and Grode, G. A. 1972. Management of hard tissue avulsive wounds and management of orofacial fractures. Report No. 3, Contract No. DADA17-69-C-9118 (October).
- (7) McCoy, L. G., Hassler, C. R., Wright, T. R., Niesz, D. E. 1974. Management of hard tissue avulsive wounds and management of orofacial fractures. Report No. 3, Contract No. DADA17-69-C-9118 (October).
- (8) McCoy, L. G., Hassler, C. R., and Niesz, D. E. 1976. Management of hard tissue avulsive wounds and management of orofacial fractures. Report No. 5, Contract No. DADA17-69-C-9118 (June).
- (9) McCoy, L. G., and Hassler, C. R. 1980. Management of hard tissue avulsive wounds and management of orofacial fractures. Report No. 6, Contract No. DADA17-69-C-9118 (August).
- (10) Hassler, C. R. and McCoy, L. G. 1981. Management of hard tissue avulsive wounds and management of orofacial fractures. Report. No. 7, Contract No. DADA17-69-C-9118 (May).
- (11) Tortorelli, A. F. and Posey, W. R. 1980. Bone ingrowth and replacement of "Ceramic in Mandibular Continuity Defects". Jour. Dental Res., 60A: 1168.
- (12) Hassler, C. R. and McCoy, L. G. 1982. Management of hard tissue avulsive wounds and management of orofacial fractures. Report No. 8, Contract No. DADA17-69-C-9118 (May).

- (13) Hassler, C. R., and McCoy, L. G. 1983. Management of hard tissue avulsive wounds and management of orofacial fractures. Report No. 9, Contract No. DAMD17-82-C-2168 (May).
- (14) Hollinger, J. 1987. Personal communication.

DISTRIBUTION LIST

1 copy	Commander U.S. Army Medical Research and Development Command ATTN: (SGRD-RMI-S) Frederick, Maryland 21701-5012
12 copies	Administrator Defense Technical Information Center ATTN: DTIC-DDA Cameron Station Alexandria, Virginia 22304-6145
1 copy	Commandant Academy of Health Sciences, U.S. Army ATTN: AHS-CDM Fort Sam Houston, Texas 78234-6100
1 copy	Dean School of Medicine Uniformed Services University of the Health Sciences 4301 Jones Bridge Road Bethesda, Maryland 20814-4799

END

DATE

FILMED

4-88

DTIC